

DOUBLY CORRUGATED COLD-FORMED ARCH ROOF PANELS. ADVANCED IDENTIFICATION OF GEOMETRICAL AND MATERIAL PROPERTIES

Ryszard WALENTYŃSKI ^a, Robert CYBULSKI ^b, Janusz MAZURKIEWICZ ^c

^a Associate Prof.; Faculty of Civil Engineering. The Silesian University of Technology, Akademicka 5, 44-100 Gliwice, Poland
E-mail address: *Ryszard.Walentynski@polsl.pl*

^b MSc Eng., PhD student; Faculty of Civil Engineering. The Silesian University of Technology, Akademicka 5, 44-100 Gliwice, Poland
E-mail address: *Robert.Cybulski@polsl.pl*

^c Dr.; Institute of Engineering Materials and Biomaterials, The Faculty of Mechanical Engineering, The Silesian University of Technology, Konarskiego 18A, 44-100 Gliwice, Poland
E-mail address: *Janusz.Mazurkiewicz@polsl.pl*

Received: 25.01.2013; Revised: 10.02.2013; Accepted: 15.03.2013

Abstract

In present days, modern building structures become much lighter than several years ago. Very often those buildings are constructed using steel thin-walled structural elements. Their shape is obtained during cold-forming prefabrication process. Such elements are very thin, have smooth surfaces and possible pressed longitudinal stiffeners. The calculation methods are known for above described cases. The question is how to calculate steel thin-walled elements with large geometrical imperfections? The easiest method is to create panel's FEM model. Due to those imperfections it is very hard to obtain a reasonable panel's geometry model. Firstly, this paper will show a way to build panel's accurate geometrical model based on 3D optical scanning method. Such model will be used in future numerical analyses. From this method, understanding of prefabrication procedure was also possible and some remarks are presented in here. Secondly, authors discuss the mechanical properties of steel sheet used for prefabrication of thin-walled panels including influence of cold forming. This paper is based on information presented during conference "New Trends in Statics and Dynamics of Buildings 2012" in Bratislava.

Streszczenie

W dzisiejszych czasach, nowoczesne konstrukcje budowlane stają się znacznie lżejsze aniżeli kilka lat temu. Bardzo często, konstrukcje te są budowane przy użyciu cienkościennych, stalowych elementów konstrukcyjnych. Ich kształt jest uzyskiwany podczas procesu gięcia na zimno. Takie elementy są bardzo cienkie, mają gładkie powierzchnie oraz możliwe są na ich powierzchni podłużne usztywnienia. Dla wyżej opisanych przypadków metody obliczeniowe są znane. Natomiast pojawia się pytanie, jak obliczać elementy cienkościenne z dużymi geometrycznymi imperfekcjami? Najprostszą metodą jest stworzenie modelu MES omawianego panelu. Ze względu na niedokładności geometryczne bardzo trudno jest uzyskać model geometryczny. Po pierwsze, artykuł ten pokazuje sposób budowania dokładnego modelu geometrycznego, opartego na metodzie przestrzennego skanowania optycznego. Taki model będzie wykorzystywany w przyszłych analizach numerycznych. Dzięki metodzie skanowania rozumiano również jak przebiega proces prefabrykacji panelu i kilka uwag zostało przedstawionych w niniejszym opracowaniu. Po drugie, autorzy omawiają właściwości mechaniczne blach, używanych do prefabrykacji cienkościennych paneli, uwzględniając wpływ gięcia na zimno. Artykuł ten bazuje na informacjach przedstawionych przez autorów publikacji na konferencji "New Trends in Statics and Dynamics of Buildings 2012" w Bratysławie.

Keywords: Doubly Corrugated; Cold-Formed; Steel; Self-Supporting; Panels; 3D Optical Scanning; Material Tests.



Figure 1. The arch buildings in Poland and South Korea: warehouses, sport gym, office building

1. INTRODUCTION

Due to today's difficult economy, cheap and short time consuming solutions for buildings industry are very desirable. One of the solutions which fulfills above requirements is the arch shaped, self-supporting building made of steel cold-formed elements. The huge advantage of such structures is that all construction process is conducted on the building site. In Fig.1 warehouses, sport gym and office building are presented as an examples of ready arch, self-supporting buildings.

Such structures are constructed from single doubly corrugated steel panels. Doubly means that prefabrication process was made in two stages: firstly shape of cross-section was obtained on the straight panel and secondly the surface transverse corrugations during arch formation. Straight and doubly corrugated panels are presented in Fig. 2. The prefabrication process is well described in [6].

Based on Eurocode3 [4] there are not straight and obvious calculation procedures for thin-walled elements with transverse geometrical imperfections. In order to find a reasonable calculation methods, in the first step very accurate panel's geometry model must be constructed. Due to very complex geometry of curved panel, it is almost impossible to build manually a numerical model which will consist of all geometrical imperfections. In order to reflect the real geometry of corrugated elements, three dimensional (3D) optical scanning method is proposed and based on that, the numerical models for finite element

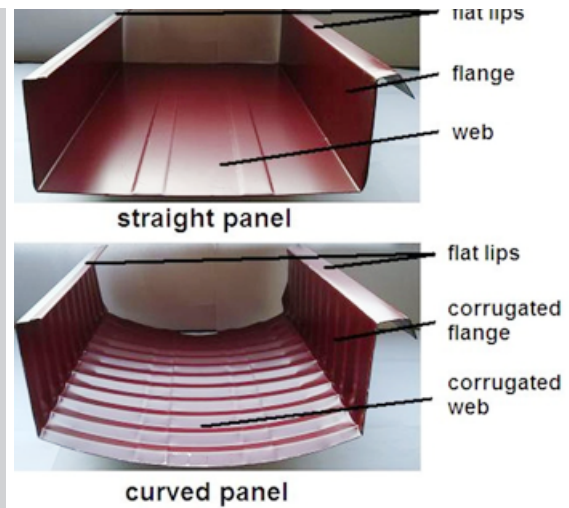


Figure 2. Straight (stage 1) and doubly corrugated (stage 2) panels



Figure 3. Arch shaped corrugated roof collapse

method (FEM) analyses will be built. Not knowing the local behavior of the doubly corrugated panels and using wrong design procedures can cause the unpredicted failure of such arch building like it is shown in Fig. 3.

2. 3D OPTICAL SCANNING

In order to scan doubly corrugated thin-walled element, 0.6 m long sample was cut from the arch of radius 5 m. Non-Contact Measurement Instrument (optical scanning device) called COMET L3D 2M was used in this case. Sample and scanning devices are presented in Fig. 4. This system converts the surface geometry into a cloud of high-density numerous points with 3D coordinates. It has been developed specifically for accurate measuring the surface geometries of items different in size or parts different in size on the same subject. The resolution and measuring range can be changed as required. In present case such device consists of 2 Mpx photo-camera with 1600×1200 resolution and projector which uses so-called structural light instead of laser and is connected to the computer.



Figure 4.
Working scanning device

Three types of camera lenses with different field of vision (FOV) equal to 100, 200 and 400 can be used for discussed scanning device. For the double corrugated panels, camera lens with FOV equal to 400 has been utilized. This choice gave the user the following accuracy of scanning:

- measuring volume in mm³: 400 × 300 × 250,
- 3D point to point distance in μm: 250,
- verified accuracy of the model after scanning in μm: 25.

Firstly, the scanning device must be calibrated. Calibration is needed due to change of camera lens and in order to accommodate the scanning device to surrounding temperature. Scanning device is positioned in front of calibrating board with in the distance of 755 mm (see Fig. 5). It is important that in the first step of calibration, scanning device and calibration board are perpendicular to each other in vertical and horizontal planes. During calibration process, location of the calibration board is changing according to given positions on the location sketch. The scanning device remains unchanged. The calibration board consists of a set of points. Scanning software, called Comet Plus which is provided by the scanner producer, knows the positions of these points. During calibration, described device is scanning the board and compares the obtained position of points with the default position from the software. If accuracy is acceptable (scan registered at least 80% of points), software allows changing the configuration of the calibration board and repeating the process.



Figure 5.
Working scanning device

Secondly, after calibration is succeeded, the main part of scanning can be started. Scanner lightens the tested object with light of specified structure. Most often the light is white or blue. The device is projecting a set of lines (fringes) with a given density on the tested object. In order to minimize the light reflection, the scanned object can be sprayed with anti-glare spray. Then information is collected about the distortion of the projected lines on the measured surface, which is due to variation of the shape of a given element. From the recorded sequence, the coordinate of a point can be calculated. Next step is data transformation called triangulation, where obtained points are changed to the triangular grid (see Fig. 6).

Triangular gird reflects much better complex shapes of elements than quadratic gird. Due to this, user is achieving a surface of 3D object. Now, the so-called “path of girds” can be created. This gird is made from triangular surfaces by connecting them in larger surfaces. The surfaces boundary is created by paths located on the scanned surface where diametrical change of geometry is obtained. Such step can be done using Geomagic software for transforming 3D scan data into highly accurate surfaces which can be exported to CAD and FEM software. Example of achieved “path of girds” and ready CAD model are shown in Fig. 7.

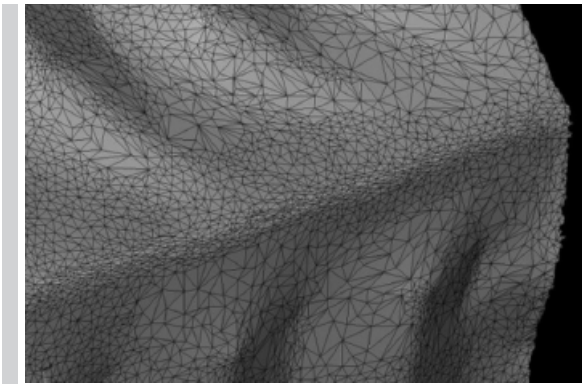


Figure 6. Triangular gird

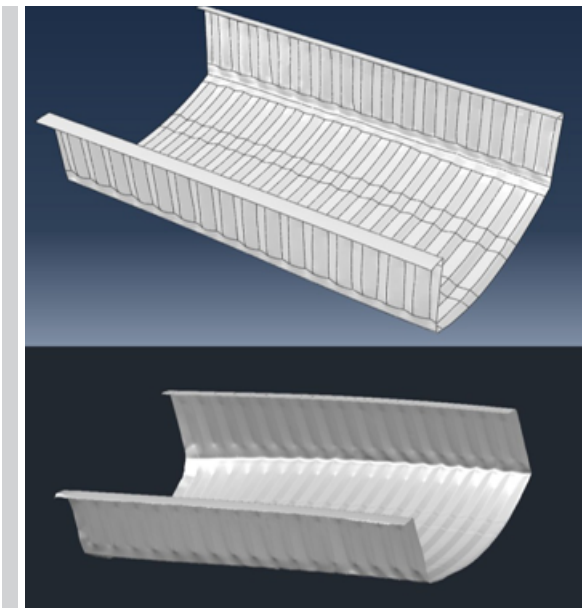


Figure 7. Geometry models: surface right after scanning, exported to CAD system

Such developed geometry model of doubly corrugated thin-walled panel is ready to export to FEM systems. The same scanning procedure was applied for samples of panels obtained from different arch radiuses. More information about scanning procedures can be found in [1, 5].

3. PREFABRICATION PROCESS

In previous section it was mentioned that scanned models are built from the cloud of points of certain coordinates. Due to this reason it was possible to measure geometry of a single corrugation of flange or web (see Fig. 8). It was observed that flange corrugation changes its height along the axis. Web corrugation has constant height. Measured values of heights are listed in Table 1.

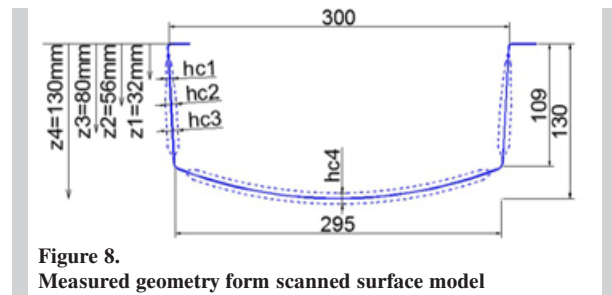


Figure 8. Measured geometry form scanned surface model

Based on that it was much easier to find out the way how the corrugations were created for different arch radiuses. In here, only the radiuses of arches equal 5 m, 7.5 m and 10 m are considered. The important unknown is a height of single corrugation cross-section, called “ h_s ”. The following parameters are given: external arch radius “ R_1 ”, height of panel’s cross-section “ h ”, corrugation width “ w_b ”. “ L_1 ” stands for the length of straight panel, “ R_2 ” is an internal arch radius and “ w_u ” is a width of flattened corrugation. These two parameters are calculated later on.

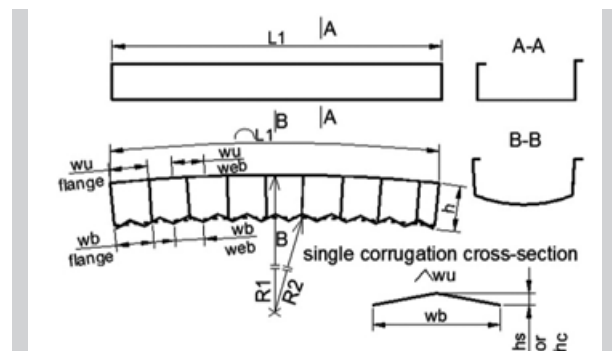


Figure 9. Geometry change during prefabrication – “gable roof” model

Table 1.
Corrugations heights-“gable roof” model

-	R ₁ [mm]	h(z) [mm]	w _b [mm]	h _s [mm]	Measured height h _c [mm]
flange	5000	32	34	1.9	2.0
		56		2.6	2.5
		80		3.1	3.1
web	5000	130	30	3.5	3.6
flange	7500	32	34	1.6	1.7
		56		2.1	2.0
		80		2.5	2.6
web	7500	130	30	2.8	2.9
flange	10000	32	34	1.4	1.5
		56		1.8	1.7
		80		2.2	2.3
web	10000	130	30	2.4	2.5

Having known parameters and based on Fig. 9, procedure for corrugation height calculation is presented:

$$\frac{R_1}{R_2} = \frac{w_u}{w_b}, \text{ where } R_2 = R_1 - h \quad (1)$$

from above it is obtained

$$w_u = w_b \frac{R_1}{R_1 - h} \quad (2)$$

Corrugation height is calculated as follows:

$$h_c = \sqrt{\frac{1}{4}w_u^2 - \frac{1}{4}w_b^2} \quad (3)$$

For the given radii and based on equations from (1) to (3), the achieved heights “h_s” of flange and web corrugations are listed in Table 1. It is observed that they are very similar to those obtained from scanning.

Described procedure is assumed on statement that the shape of corrugation cross-section is close to “gable roof”. Now similar procedure was established but with assumption that the shape of corrugation cross-section is close to a half wave of sine curve.

Knowing value of “w_u” from equations (1) and (2), the height of single corrugation can be calculated based on Fig. 10 and the function of a half wave of sine curve presented below:

$$f(x) = h_c \sin\left(\frac{\pi x}{w_b}\right) \quad (4)$$

The length of a half wave is calculated as follows:

$$w_u = \int_0^{w_b} \sqrt{1 + f'(x)^2} dx \quad (5)$$

Solving equation (5) for “h_c” gives the heights of sin-

gle corrugations of sinusoidal shape. The results are listed in Table 2.

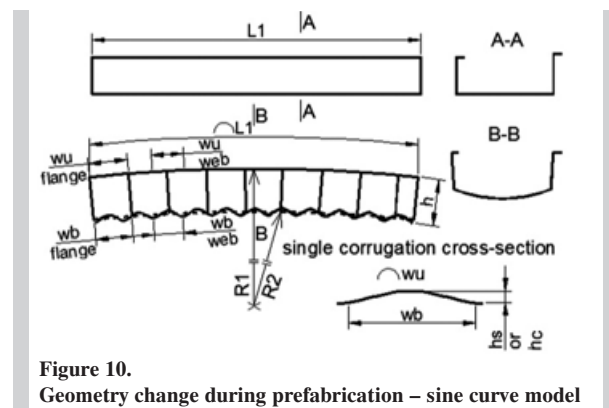


Figure 10.
Geometry change during prefabrication – sine curve model

In a very few publications [7, 8], authors were trying to establish what corrugations shape should be applied for doubly corrugated panels investigations. Comparing results from Table 1 and 2 it can be stated that the values heights of corrugations shaped as “gable roof” are closer to heights achieved from scanning. Looking at the cut through corrugations (Fig. 11) it seems that assuming the shape as similar to the shape of “gable roof” is accurate enough.

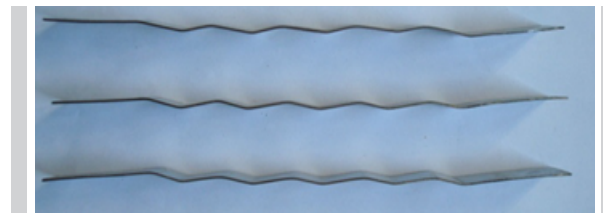


Figure 11.
Shapes of corrugations

Table 2.
Corrugations heights-sine curve model

-	R_1 [mm]	$h(z)$ [mm]	w_b [mm]	h_s [mm]	Measured height h_c [mm]
flange	5000	32	34	1.7	2.0
		56		2.3	2.5
		80		2.8	3.1
web	5000	130	30	3.2	3.6
flange	7500	32	34	1.4	1.7
		56		1.9	2.0
		80		2.3	2.6
web	7500	130	30	2.6	2.9
flange	10000	32	34	1.3	1.5
		56		1.7	1.7
		80		2.0	2.3
web	10000	130	30	2.2	2.5

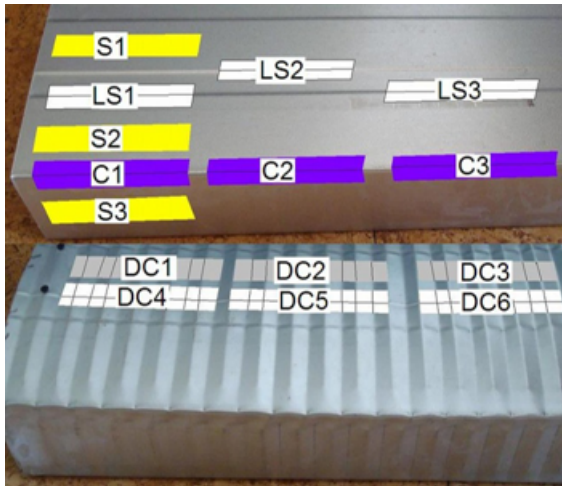


Figure 12.
Tests pieces locations

4. MATERIAL TESTS

Previous sections of this paper were focused on the doubly corrugated panels' geometry. This section will discuss mechanical properties of metal sheet used for panels' prefabrication including influence of cold forming.

The material test (static tensile testing at ambient temperature) was conducted on test pieces cut out from straight and doubly corrugated panels (called also curved panels). Locations of cutouts are presented in Fig. 12. In total 15 samples of different types were used for the material test purposes. Geometry of these test pieces is presented in Fig. 13 where L_c is the sample's parallel length and L_0 is original gauge length. The test pieces were achieved by contour grinding where rolled

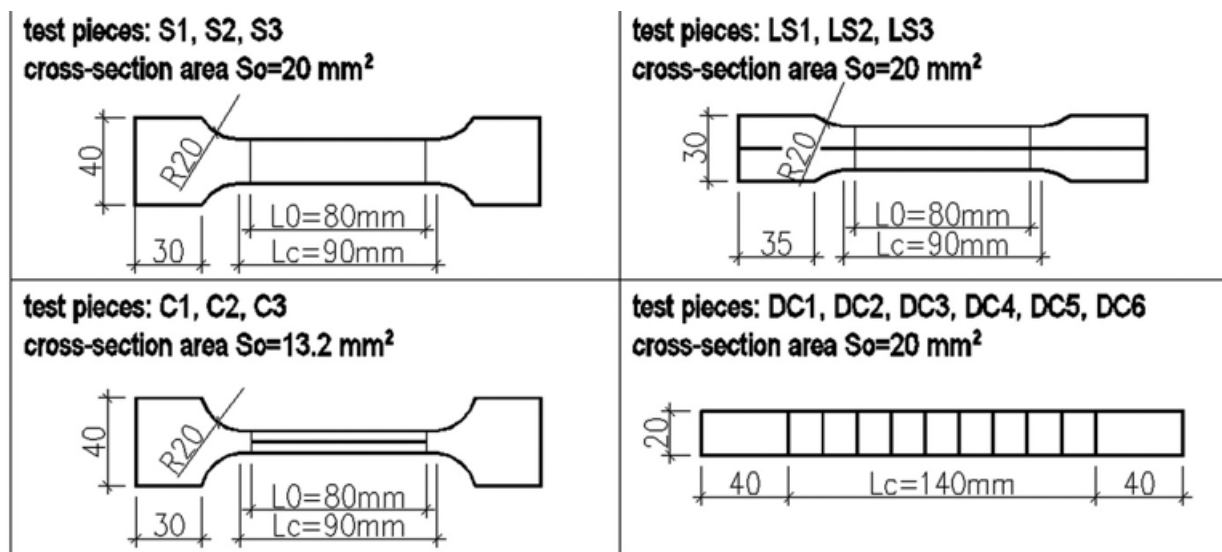


Figure 13.
Tests pieces geometries

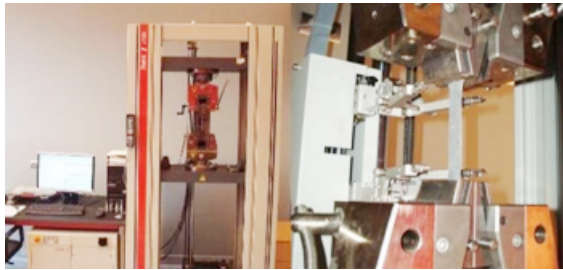


Figure 14.
Testing machine

surface of samples was not machine treated. Thickness of each sample was equal to 1 mm.

According to panels producers, straight and corrugated panels were fabricated from the steel sheet of grade S320GD+ZA. This steel grade is commonly used for cold forming purposes and it is continuously hot-dipped zinc-aluminum (ZA) coated steel sheet. For such steel grade EC3 [4] recommends minimum value of yield strength $f_y=320$ MPa, tensile strength $f_u=390$ MPa and the minimum percentage elongation after fracture $A=18\%$.

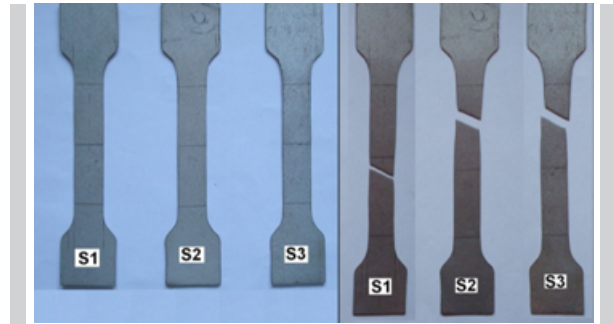


Figure 15.
Flat test pieces

Material testing machine with central ball-lead screw called Zwick/Z100 was used. Such experimental device is controlled by the test Xpert software. The test rate was established to a strain rate equal to 0.008 s^{-1} . The experimental machine is presented in Fig. 14. Sample installed in the machine clamps with the view on the extensometer is also shown in Fig. 14.

The main purposes of these material tests are to see how the cold forming influences the mechanical properties of steel sheet and what mechanical properties should be used for doubly corrugated panels.

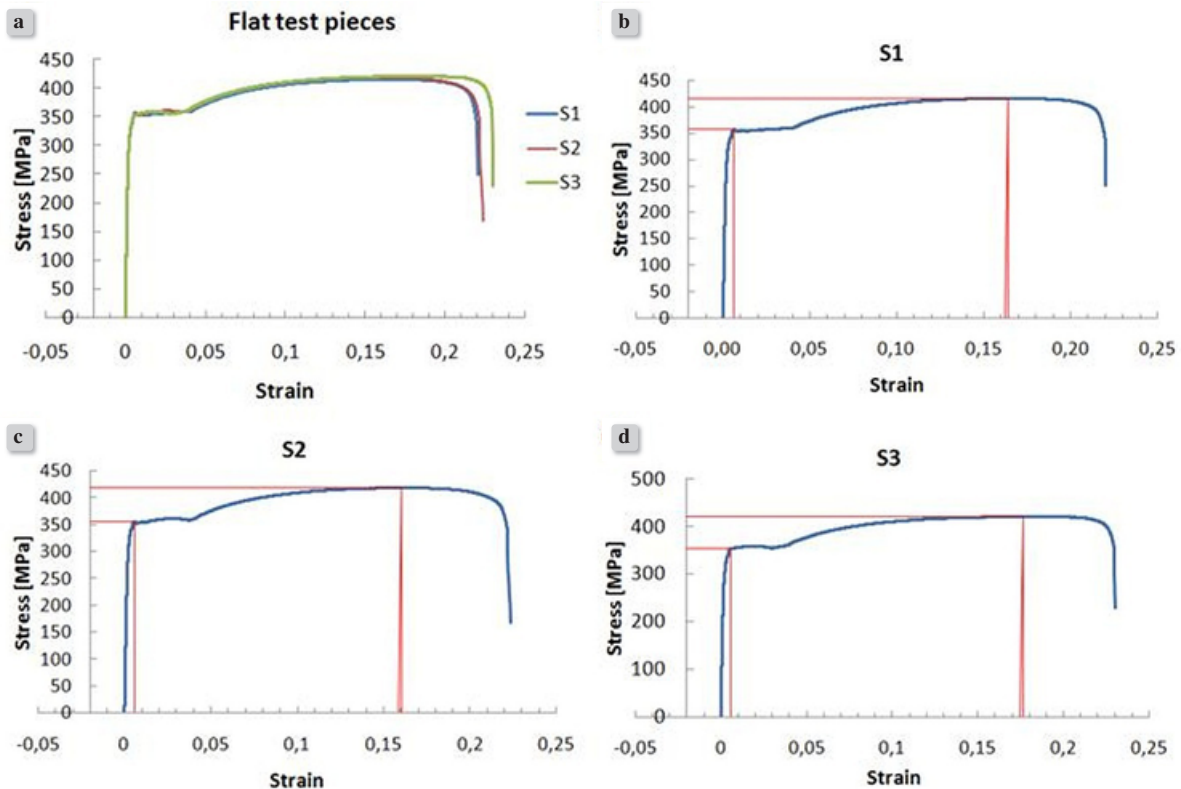


Figure 16.
Stress-strain curves obtained from flat test pieces

Table 3.
Mechanical properties of flat tests pieces

Name	Modulus of Elasticity, E [GPa]	Upper yield strength R_{eH} [MPa]	Tensile strength R_m [MPa]	Percentage total elongation at maximum force A_{gt} [%]	Percentage elongation after fracture A_{test} [%]
S1	203.1	356.5	415.4	16.39	22.03
S2	205.4	356.4	418.6	15.88	22.34
S3	201.3	353.0	420.6	17.60	22.98
mean value	203.3	355.3	418.2	16.62	22.45

4.1. Flat pieces “S”

The geometry of samples was established in accordance with Polish Standards PN-EN ISO 6892-1 [2]. The test procedure including the speed of strain rate or the gauge length was also prepared according to the same code. Three flat pieces were tested and achieved results have quantitative meaning for described research purposes.

Flat samples before and after testing are shown in Figure 15. It can be observed that the material break took place between two external lines which mark the measuring gauge length (80mm).

Figure 16 a) presents the test results achieved from three samples. Vertical axis stands for values of tensile stresses and horizontal for values of strains obtained during extensometer work. From this stress-strain graphs, it can be stated that samples were investigated with very similar accuracy. From Figure 16 b), c), d), where stress-strain graphs are separately presented for each test piece, it is observed that the shapes of curvatures have typical shape which can be obtained from such tests with visible upper yield strength value and with an apparent yielding plateau.

The obtained mechanical properties of the steel sheet such as modulus of elasticity, upper yield strength, tensile strength, percentage total elongation at maximum force and percentage elongation after fracture are listed in Table 3. Due to the fact that only three samples were tested, for results comparison purposes, the mean values of each properties are considered. All these values fulfill requirements for steel grade S320GD+ZA i.e.

$$f_y = 320 \text{ MPa} < R_{eH} = 355.3 \text{ MPa},$$

$$f_u = 390 \text{ MPa} < R_m = 418.2 \text{ MPa} \text{ and}$$

$$A = 18\% < A_{test} = 22.45\%.$$

Modulus of elasticity was obtained from the slope of a section achieved as a linear regression of values of stresses and strains in the stresses range from 15 MPa to 250 MPa. This range was chosen because the increments of stresses and strains were almost constant.

4.2. Flat test pieces with longitudinal stiffeners “LS”

The dimensions of samples and test procedure were adopted from the same standards as in case of flat test pieces. Three samples were considered with longitudinal stiffener (cold work along longitudinal axis of test piece). There are two reasons why the results obtained for such samples can be only treated in qualitative way:

- Polish Standard PN-EN ISO 6892-1[2] shows the samples geometry of steel sheets only for cases where surface is plane- in this case longitudinal stiffener is taken into account,
- It was very hard to obtain the samples geometry with longitudinal stiffener placed exactly along their longitudinal axes, so this tensile test is saddled with imperfection which can cause eccentricity in applied tensile force.

Test pieces before and after testing are shown in Figure 17. The material break took place in the range of gauge length (80 mm).

Fig. 18 presents stress-strain graphs where a) covers all three samples and b), c), d) shows stress-strain

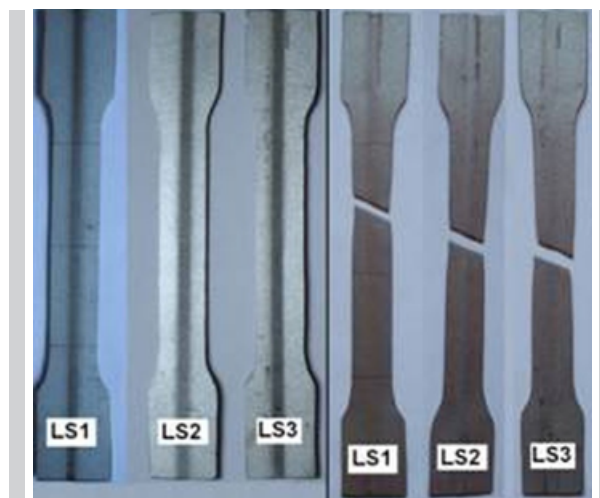


Figure 17.
Flat test pieces with longitudinal stiffeners

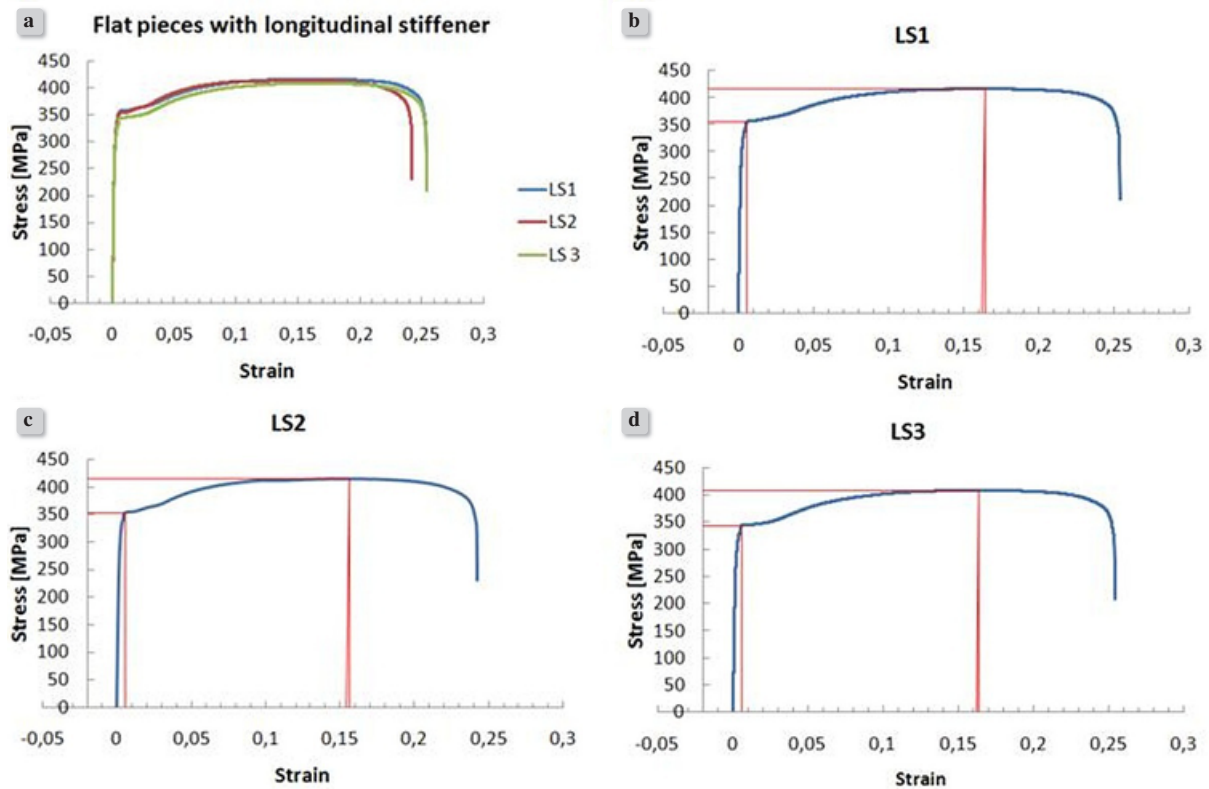


Figure 18. Stress-strain curves obtained from flat test pieces with longitudinal stiffeners

Table 4. Mechanical properties of flat tests pieces with longitudinal stiffeners

Name	Modulus of Elasticity, E [GPa]	Upper yield strength R_{eH} [MPa]	Tensile strength R_m [MPa]	Percentage total elongation at maximum force A_{gt} [%]	Percentage elongation after fracture A_{test} [%]
S1	200.1	355.7	416.6	16.41	25.41
S2	204.8	353.1	414.4	15.63	24.23
S3	204.1	343.6	408.6	16.38	25.38
mean value	203.0	350.8	413.2	16.14	25.01

relations for each sample separately. It is observed that all three tensile tests on samples “LS” were carried out with similar accuracy. It is also observed that longitudinal stiffener does not influence much the values of mechanical properties comparing with flat samples “S”. The reason for this is that area of the stiffener is much smaller than the flat area of considered single sample. Of course such longitudinal cold works influence the course of stress-strain graphs. In Fig. 18 b), c), d) after passing the value of upper yield strength, there is a short yield point extension zone, after which stresses increase to the value of tensile

strength. In case of flat samples (Fig. 16 b), c), d)) the yield point extension zone is more clear and it takes some time to start for stresses to increase in order to reach the value of tensile strength.

Table 4 presents results obtained from tensile tests of LS samples. These values of mechanical properties of steel sheets with longitudinal stiffeners “LS” do not differ much from values obtained for flat samples “S”. Like for previous example, modulus of elasticity was obtained from the slope of a section achieved as a linear regression of values of stresses and strains in the stresses range from 15 MPa to 250 MPa.

Table 5.
Mechanical properties of corner tests pieces

Name	Modulus of Elasticity, E [GPa]	Upper yield strength R_{eH} [MPa]	Tensile strength R_m [MPa]	Percentage total elongation at maximum force A_{gt} [%]	Percentage elongation after fracture A_{test} [%]
S1	208.8	431.9	487.6	12.55	18.51
S2	208.4	438.9	490.6	12.20	18.19
S3	208.1	412.4	480.1	11.77	17.53
mean value	208.4	427.7	486.1	12.77	18.08

4.3. Corner tests pieces “C”

Like in previous case, the test procedure was adopted from the Polish Standard PN-EN ISO 6892-1[2]. The shape of corner test pieces was based on a quasi flat part near the corner of a corrugated panel. The width of this part is equal around 6.6 mm. Even though the corner samples were cut out from the straight panel, due to minimization of geometry and work quality imperfections, the total width of two almost perpendicular parts of the corner is equal 13.2 mm (2×6.6 mm). The gripped ends were straightened in order to prevent a slide of test pieces in the machine clamps.

Three samples, presented in Fig. 19, were considered during tensile test. The material break took place in the range of gauge length (80 mm).



Figure 19.
Corner test pieces

Fig. 20 presents stress-strain graphs where a) covers all three samples and b), c), d) shows stress-strain relations for each sample separately. It is observed that all three tensile tests on samples “C” were carried out with similar accuracy. From these graphs, it can be concluded that the cold bend of steel sheet in order to obtain a corner, considerably influences mechanical properties of this steel sheet. This is a known phenomenon in which the yield strength and tensile strength increase and due to steel hardening the values of strains decrease. The courses of obtained stress-strain curves have a typical shape where proof yield strength at a strain equal 0.002 must be found. There is a clear, visible change of a stress-strain curve course comparing to previous examples. Due to a reason that only three corner samples were considered and their shapes are not covered by any standards or codes, the obtained results have only usability in this very particular case. Obtained results from corner tests pieces will be used in further investigations and they will be verified by the panels compression tests. The obtained mechanical properties of the corner steel sheet are listed in Table 5. Modulus of elasticity was obtained from the slope of a section achieved as a linear regression of values of stresses and strains in the stresses range of 50 MPa to 300 MPa. This range was chosen because the increments of stresses and strains were almost constant.

4.4. Test pieces with transverse corrugations “DC”

The dimensions of samples and test procedure once again were adopted from the standards PN-EN ISO 6892-1 [2]. Six samples were considered and obtained results have only qualitative meaning due to:

- unrepetitive geometry of the corrugations- each corrugation has different dimensions so in order to obtain results with quantitative meaning much more samples are needed,
- production possibility of test pieces – the geometry

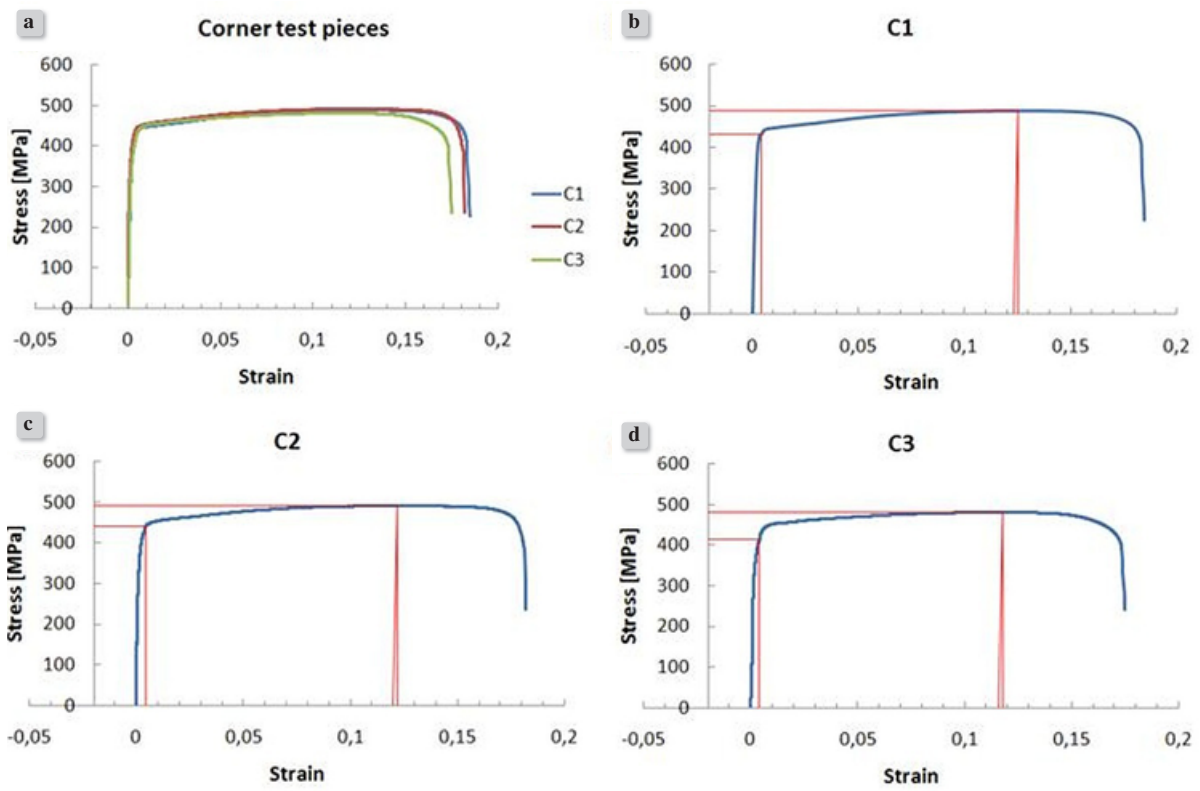


Figure 20. Stress-strain curves obtained from corner test pieces

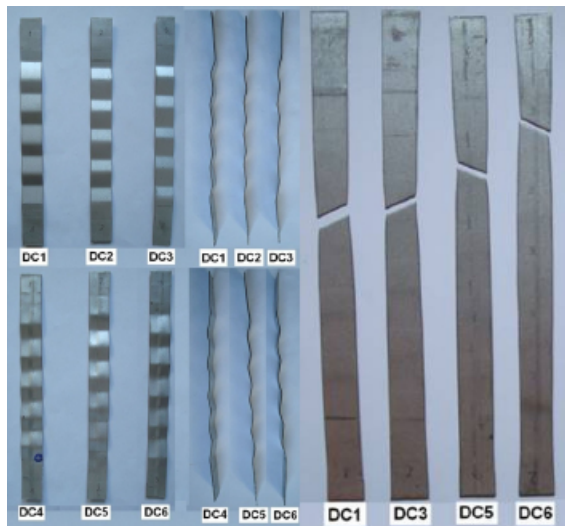


Figure 21. "DC" test pieces

of corrugated panels is very complex so it was very hard to achieve samples with parallel and straight edges,

c) test machine traverse displacement measuring

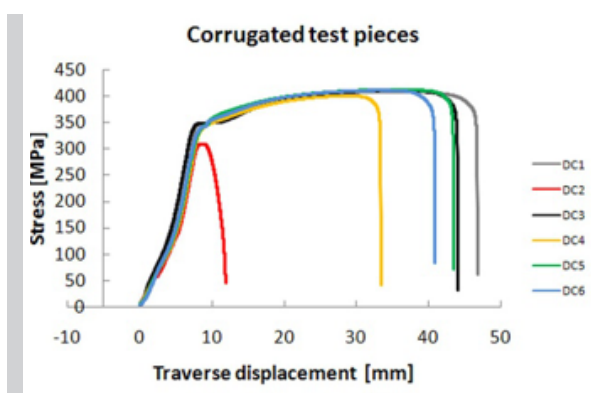


Figure 22. "DC" test pieces – test results

instead of strains obtained from extensometer – due to corrugations geometry it was impossible to install properly the extensometer,

d) repetitive results – only achieved results from four samples were possible to compare with each other.

Six test pieces before and four test pieces after testing are shown in Figure 21. The material break took place in the range of gauge length (140 mm).

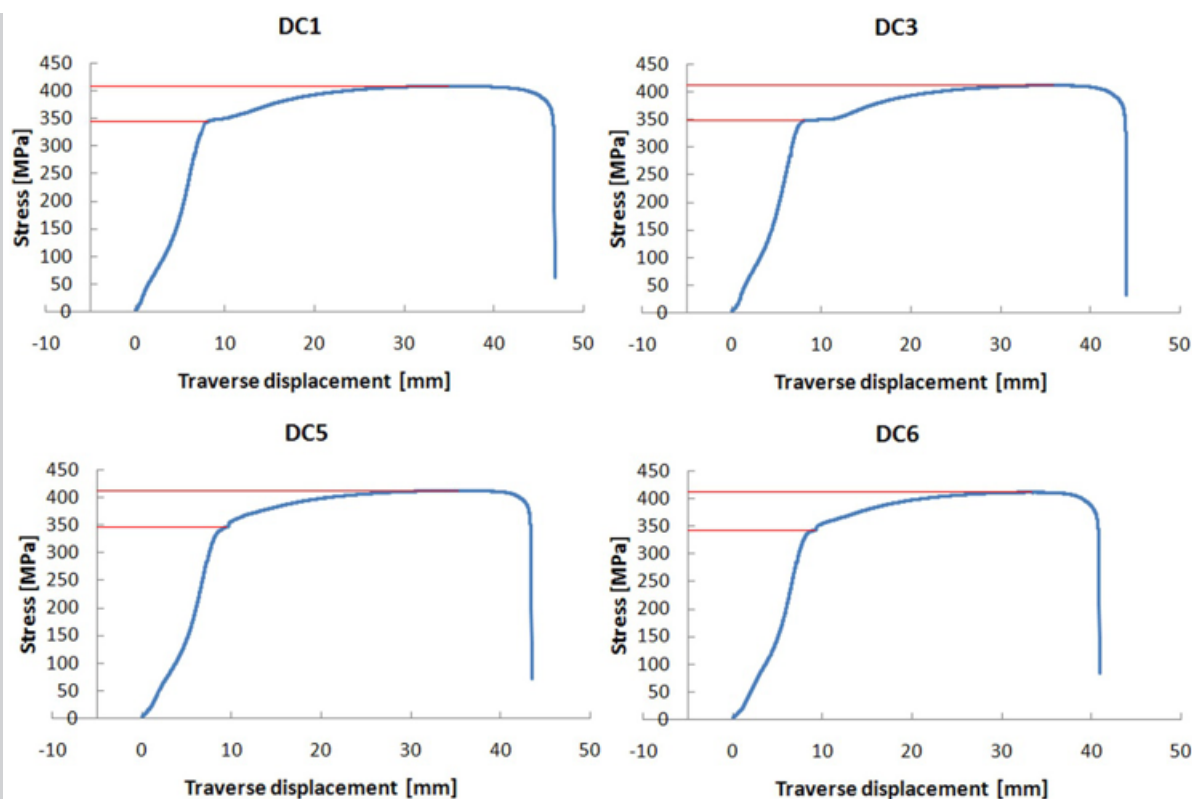


Figure 23.
Stress-displacement curves for DC1, DC3, DC5 and DC6 samples

In Fig. 22 the stress-displacement curves obtained from all six samples are presented. It is obvious that results from samples DC2 and DC4 are not taken into any consideration.

Test pieces DC1 and DC3 are cut from corrugated panel from places without longitudinal stiffener. DC5 and DC6 are with the longitudinal stiffener. From Fig. 23 it can be observed that this stiffener like in case of flat samples with longitudinal stiffener has influence only on the stress-displacement curve shape. There is a short yield point extension zone, for samples DC5 and DC6 and more clear yield point extension zone for samples DC1 and DC 3. Once again longitudinal stiffener does not influence much the values of mechanical properties (see Table 6).

For corrugated test pieces it can be concluded that geometrical imperfections such as transverse corrugations do not influence the important values of mechanical properties such as upper yield strength and tensile strength obtained from the tensile material test in the longitudinal direction i.e. in the direction transverse to the corrugations axes.

Table 6.
Mechanical properties of corrugated tests pieces

Name	Upper yield strength R_{eH} [MPa]	Tensile strength R_m [MPa]
DC1	344.5	408.4
DC3	347.2	411.5
DC5	346.1	412.2
DC6	343.0	411.1
mean value	345.2	410.8

4.5. Nominal vs. true stress and strain relations

The previous subchapter presents results of engineering stresses and strains obtained for the material tensile tests. The value of stress is calculated as force per unit undeformed area and value of strain as length change per unit undeformed length. The engineering stress in the metal as it is necking is much lower than the material ultimate strength. In order to find values of stresses and strains which are closer to reality the concept of true stresses and strains must be introduced.

Firstly, from obtained earlier results, interesting for the future numerical analysis, values of stresses and strains are chosen. Based on experimental investigation described in previous subchapter, for both

straight and corrugated panels the following values of steel sheet mechanical properties are chosen:

- near the corners: modulus of elasticity $E=208.4$ GPa, proof strength $R_{p0.2}=427.7$ MPa, tensile strength $R_m=486.1$ MPa, Percentage total elongation at maximum force $A_{gt}=12.77\%$,
- remained surface: modulus of elasticity $E=203.3$ GPa, proof strength $R_{eH}=355.3$ MPa, tensile strength $R_m=418.2$ MPa, Percentage total elongation at maximum force $A_{gt}=16.62\%$,

Such choice of values was justified by the following conditions:

- only flat samples were totally investigated according to Polish Standards PN-EN ISO 6892-1 (consistent samples' shape and test procedure) so obtained results can be assumed as quantitative values,
- other results based on LS, C, DC samples have only qualitative meaning, even that values obtained from corner samples are taken into consideration because they seems to be reasonable (the values of yield strength and tensile strength are higher than those one achieved for flat samples, and percentage elongation is shorter then in case of flat samples).

So usage of engineering stresses and strains is favorable when change of samples dimensions is very small. During bigger plastic strains, more appropriate is to use so called true stresses and strains.

The true stress is defined as follows:

$$\sigma = \frac{F}{A} \quad (6)$$

where F is the force in the material and A is the current area. The true strain has the following form:

$$\varepsilon = \sum \frac{\Delta l_j}{l_j} \quad (7)$$

where change of length is measured in small increments $\Delta l_1, \Delta l_2, \Delta l_3$ etc. and current gauge length l_1, l_2, l_3 etc. is used for calculation of strains in each increment.

When Δl_j are very small, we can write:

$$\varepsilon = \int_{l_0}^l \frac{dl}{l} = \ln\left(\frac{l}{l_0}\right) \quad (8)$$

where l is the current length ($l=l_0+\Delta l$), l_0 is the original length. ε is also called the logarithmic strain or Hencky strain.

Now, knowing that engineering strain is equal to

$$\varepsilon_{eng} = \frac{\Delta l}{l_0} \quad (9)$$

Based on equations (8) and (9) we obtain:

$$\varepsilon = \ln\left(\frac{l_0 + \Delta l}{l_0}\right) = \ln\left(1 + \frac{\Delta l}{l_0}\right) = \ln(1 + \varepsilon_{eng}) \quad (10)$$

If during a deformation the volume of the sample is conserved, i.e.

$$A_0 * l_0 = A * l \quad (11)$$

where A_0 is original area of the cross-sections, we can relate the current area to the original area by

$$A = A_0 * \frac{l_0}{l} \quad (12)$$

Table 7.
True values of stresses and strains obtained from corner samples

Corner sample					
	Engineering stress [MPa]	Engineering strain	True stress [MPa] Eq.13	True strain Eq.10	Plastic strain Eq.14
At the point of f_y	427.7	0.0021	428.6	0.0021	0
At the point of f_u	486.1	0.128	548.3	0.120	0.118

Table 8.
True values of stresses and strains obtained from flat samples

Flat sample					
	Engineering stress [MPa]	Engineering strain	True stress [MPa] Eq.13	True strain Eq.10	Plastic strain Eq.14
At the point of f_y	655.6	0.0017	355.9	0.0017	0
At the point of f_u	418.2	0.166	487.6	0.154	0.152

Table 9.
True values of stresses and strains which will be used for numerical analyses purposes

	f_y [MPa]	Corresponding plastic strain	f_u [MPa]	Corresponding plastic strain
Corner regions	428.6	0	548.3	0.118
Rest of the regions	355.9	0	487.6	0.152

Substituting equation (12) in to (6) we get

$$\sigma = \frac{Fl}{A_0 l_0} = \sigma_{eng} \left(\frac{l}{l_0} \right) = \sigma_{eng} \left(\frac{l_0 + \Delta l}{l_0} \right) = \sigma_{eng} (1 + \varepsilon_{eng}) \quad (13)$$

Based on EC3 [3], yield strength f_y is equal to yield strength of product standard (R_{eH} , $R_{p0.2}$) and ultimate strength f_u is equal to tensile strength of a product (R_m). Converted values of needed mechanical properties from engineering to true one are listed in Table 7 and 8 for corner sample and flat sample respectively. At the point of yield strength f_y there is no plastic strain, so engineering strain is an elastic strain based on Hook theory ($\varepsilon_{eng}^{el} = \frac{\sigma_{eng}}{E}$) In other cases plastic strain is calculated from

$$\left(\varepsilon_{eng}^{el} = \frac{\sigma_{eng}}{E} \right) \quad (14)$$

where ε^t is true total strain and at the point of ultimate strength is related to A_{gt}

4.6. Distribution of values of mechanical properties on the panels surface

Based on material tests and conversion from engineering to true values of stresses and strains, the assumed distribution of mechanical properties for straight and curved panels is presented in Fig. 24 and 25 respectively. Red color represents corner regions and blue the rest of the regions. Needed values for future numerical analysis in Abaqus software are listed in Table 9.



Figure 24.
Straight panel – colored regions for mechanical properties description

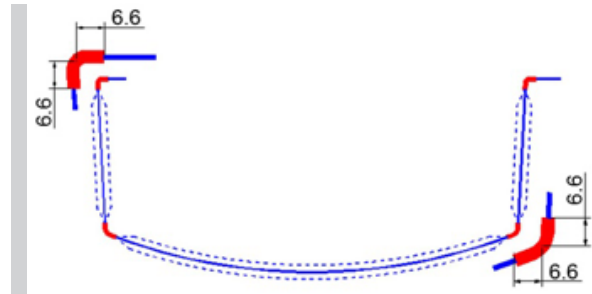


Figure 25.
Corrugated panel – colored regions for mechanical properties description

5. CONCLUSIONS

This paper discusses the process of collection of needed data for FEM model creation of complex shape of cold-formed, thin-walled, doubly corrugated panels which are used for construction of arch shaped self supporting roofs and buildings. Such model consists of geometry and material models.

Firstly, paper briefly presents the way of creation of geometry model of thin-walled elements with complex geometry. Such method is based on 3D optical scanning. Obtained model reflects the real geometry of doubly corrugated panel with very good accuracy and can be used for future numerical analyses to investigate its local behavior. Scanned model gave information about single corrugation dimensions. This was used to build analytical procedure for corrugation height estimation. Two types of corrugations shapes were assumed: “gable roof” shape and as a half wave of sine curve. It was stated that height of a single corrugation based on “gable roof” shape is similar to one achieved from scanning. The values of corrugations heights will be important for future analytical calculation of doubly corrugated panel axial and flexural stiffness.

Secondly, authors present the material tests conducted on test pieces cut out from straight and corrugated panels. This part was important due to estimation of mechanical properties of metal sheet used for panels prefabrication including influence of cold form-

ing. It was stated that from engineering point of view transverse corrugations do not influence necessary values of mechanical properties. Obtained values from test will be used in future numerical analyses.

As for the future work, FEM model will be constructed based on described above models and numerical analyses such as linear and non-linear local stability will be run in Abaqus commercial FEM system. As a result an effective cross-section for doubly corrugated panels will be established. This cross-section is necessary for design procedures of structures made of thin-walled including cold formed elements.

ACKNOWLEDGEMENT

This paper has been financed by National Science Centre based on grant no. DEC-2011/01/N/ST8/03552. Co-author of this paper R. Cybulski is a scholar under the project “DoktoRIS – scholarship program for innovative Silesia” co-financed by European Union under the European Social Fund.

REFERENCES

- [1] *Kus A.*; Implementation of 3D Optical Scanning Technology for Automotive Applications. *Sensors*, No. 9, 2009, p.1967-1979
- [2] EN ISO 6892-1: Metallic materials – Tensile testing – Part 1: Method of test at room temperature, 2009
- [3] Eurocode 3: Design of steel structures- Part 1-1: General rules and rules for buildings, EN 1993-1-1, 2007
- [4] Eurocode 3: Design of steel structures- Part 1-3: General rules- Supplementary rules for cold-formed members and sheeting. EN 1993-1-5, 2006
- [5] *Li L., Schemenauer, N., Peng X., Zeng Y., Gu P.*; A reverse engineering system for rapid manufacturing of complex objects. *Robotics and Computer-Integrated Manufacturing*, No.18, 2002, p.53-67
- [6] *Walentyński R., Cybulski R., Kozieł K.*; Achilles’ heel of the ABM 120 double corrugated profiles. *New Trends in Statics and Dynamics of Buildings*, 25-28. Slovakia University of Technology in Bratislava, Bratislava, 2011
- [7] *Wu L.L., Gao X. N., Shi Y. J., Wang Y.Q.*; Theoretical and Experimental Study on Interactive Local Buckling of Arch-Shaped Corrugated Steel Roof. *Steel Structures*, No.6, 2006, p.45-54
- [8] *Xuanneng G., Haoming Z., Huihu Z.*; Research on Ultimate Bearing Capacity of Trapezium Corrugated Plate – Assemblies Arch Steel Roof. *IEEE*, 2011, p.2553-2556

